

# Amplifying ultraweak transitions in collective systems via quantum interference

Ni Cui<sup>1,2,3,\*</sup> and Mihai A. Macovei<sup>1,4,†</sup>

<sup>1</sup>*Max-Planck-Institut für Kernphysik,*

*Saupfercheckweg 1, D-69117 Heidelberg, Germany*

<sup>2</sup>*Siyuan Laboratory, Guangzhou Key Laboratory of*

*Vacuum Coating Technologies and New Energy Materials,*

*Department of Physics, Jinan University, Guangzhou 510632, China*

<sup>3</sup>*Guangdong Provincial Key Laboratory of Optical Fiber Sensing and Communications,*

*Jinan University, Guangzhou 510632, China*

<sup>4</sup>*Institute of Applied Physics, Academy of Sciences of Moldova,*

*Academiei str. 5, MD-2028 Chişinău, Moldova*

(Dated: October 8, 2021)

## Abstract

We investigate laser-induced quantum interference phenomena in superradiance processes and in an ensemble of initially excited  $\Lambda$ -type closely packed three-level emitters. The lower doublet levels are pumped with a coherent laser field. Due to constructive quantum interference effects, the superradiance occurs on a much weaker atomic transition which is not the case in the absence of the coherent driving. This result may be of visible relevance for enhancing ultraweak transitions in atomic or atomic-like systems, respectively, or for high-frequency lasing effects.

*Introduction:* Vacuum induced correlations among closely spaced quantum emitters forming an ensemble lead to significant changes in the quantum dynamics [1–7]. In this context, the superradiance - an already well-known phenomenon - emphasizes the fast decay of an initially excited cooperative system as well as an enhanced radiation intensity, respectively. An enormous amount of experimental and theoretical works were performed with respect to this issue and superradiance behaviors were found in a wide range of different systems and for various applications [8–17]. The collective quantum dynamics can be manipulated by applying external coherent laser sources. Particularly, triggering of the superradiance phenomenon nicely occurs in a three-level Vee-type atomic ensemble when an external coherent field pumps one of the atomic transitions [18]. In a somehow related setup, superfluorescence without inversion was shown to occur as well [19], see also [20]. One may anticipate cooperative effects in novel systems because x-ray free-electron lasers may accelerate the decay of a nuclear isomer [21]. Furthermore, in a large ensemble of nuclei operating in the x-ray regime and resonantly coupled to a common cavity environment, two fundamentally different mechanisms related to cooperative emission and magnetically controlled anisotropy of the cavity vacuum have been responsible for fascinating effects mainly related to quantum interference phenomena [22]. Actually, these effects originate from indistinguishability of the corresponding transition pathways [5, 6, 22, 23].

Interfering transition amplitudes can be used in principle to detect weak atomic interactions like measurements of magnetic dipole interactions, quadrupole interactions or weak atomic transitions occurring, for instance, because of parity violation effects as well as to identify various nonlinear transition channels [24–27]. Furthermore, ultranarrow absorption lines due to electromagnetically induced transparency phenomenon were shown to be very useful for high-accuracy optical clocks [28]. Quite recently, superradiance on the millihertz linewidth strontium clock transition was shown to occur in [29]. This was achieved with the help of an optical cavity which triggered the superradiance on the ultraweak transition. Somehow related, prospects for millihertz-linewidth lasers were suggested too in [30].

Under these circumstances, we discuss here a setup where weak or ultraweak decaying transitions can be significantly enhanced in an initially excited ensemble of few-level collectively interacting  $\Lambda$ -type atoms. Notably, the effect arises due to quantum interference phenomena among different decaying pathways which are induced by the coherent pumping of the two lower levels. The rapid time-evolution on a ultraslow atomic transition is deter-

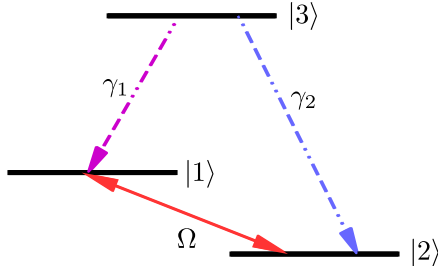


FIG. 1: (Color online) The energy levels of the  $\Lambda$ -type three-level system.  $\gamma_1$  and  $\gamma_2$ ,  $\gamma_1 \gg \gamma_2$ , are the single-atom spontaneous decay rates on transitions  $|3\rangle \rightarrow |1\rangle$  and  $|3\rangle \rightarrow |2\rangle$ , respectively. The coherent laser field drives the  $|1\rangle \leftrightarrow |2\rangle$  transition with  $\Omega$  being the corresponding Rabi frequency.

mined by the fast decay rate on another transition of the  $\Lambda$  sample. Moreover, the effect is of the cooperative nature and it is absent in excited single-atom systems or independent atomic ensembles, respectively. Particularly, (i) we have found that the superradiance on the ultraweak transition may take place when there are more atoms on the ground state than in the excited one; (ii) the superradiance peak occurs when the population of the excited level is trapped and almost constant during a short time which is distinct from the standard superradiance phenomenon where its time-dependent intensity relies on the fast population slope; (iii) quantum coherences induced by the coherent pumping are responsible for superradiant population transfer on ultraweak transition as well as among the lower sublevels during the superradiant burst. As possible applications of our results we suggest enhancing dipole-forbidden or any other ultraweak transitions, or in quantum clocks atomic systems, respectively, as well as for high-frequency lasing.

*Analytical framework:* We consider an initially excited ensemble of  $N$  identical  $\Lambda$ -type three-level emitters each consisting of states  $|1\rangle$ ,  $|2\rangle$  and  $|3\rangle$ , as depicted in Figure 1. The lower doublet transition  $|2\rangle \leftrightarrow |1\rangle$  is resonantly driven by a coherent laser field. The emitters can decay via a fast dipole-allowed  $|3\rangle \leftrightarrow |1\rangle$  transition as well as through a slow or ultraslow  $|3\rangle \leftrightarrow |2\rangle$  atomic transition, respectively, due to coupling with the environmental vacuum modes. The interparticle separations are of the order of relevant emission wavelengths of the system, or smaller, and in this way the atomic sample acquires a cooperative nature.

In the usual mean-field, Born-Markov and rotating-wave approximations, our model is

described by the following master equation [2–6]

$$\begin{aligned} \dot{\rho}(t) + i\Omega \sum_{j=1}^N [S_{12}^{(j)} + S_{21}^{(j)}, \rho] = & - \sum_{j,l=1}^N \{ \gamma_{jl}^{(1)} [S_{31}^{(j)}, S_{13}^{(l)} \rho] \\ & + \gamma_{jl}^{(2)} [S_{32}^{(j)}, S_{23}^{(l)} \rho] \} + \text{H.c.} \end{aligned} \quad (1)$$

Here  $\Omega$  is the corresponding Rabi frequency, while  $\gamma_{jl}^{(s)} \equiv \gamma_s \left[ \aleph_{jl}^{(s)} + i\Omega_{jl}^{(s)} \right]$  ( $s \in \{1, 2\}$ ) are the collective parameters with  $\aleph_{jl}^{(s)}$  and  $\Omega_{jl}^{(s)}$  describing the mutual interactions among emitter-pairs  $\{j, l\}$ . For dipole-allowed transitions, for instance, one has  $\aleph_{jl}^{(s)} = \sin(\omega_{3s} r_{jl}/c)/(\omega_{3s} r_{jl}/c)$  and  $\Omega_{jl}^{(s)} = -\cos(\omega_{3s} r_{jl}/c)/(\omega_{3s} r_{jl}/c)$  where we have averaged over all dipole orientations, whereas  $r_{jl} = |\vec{r}_j - \vec{r}_l|$  are the inter-particle intervals between the  $j$ th and the  $l$ th emitters, respectively [2–9]. Further,  $\omega_{\alpha\beta}$  with  $\{\alpha, \beta\} \in \{1, 2, 3\}$  is the frequency of the  $|\beta\rangle \leftrightarrow |\alpha\rangle$  atomic transition.  $S_{\alpha\beta}^{(j)} = |\alpha\rangle_{jj}\langle\beta|$  represents the population of the state  $|\alpha\rangle$  in the  $j$ -th atom, if  $\alpha = \beta$ , or the transition operator from  $|\beta\rangle$  to  $|\alpha\rangle$  of the  $j$ -th atom when  $\alpha \neq \beta$ . The atomic operators obey the commutation relations  $[S_{\alpha\beta}^{(j)}, S_{\beta'\alpha'}^{(l)}] = \delta_{jl} (\delta_{\beta\beta'} S_{\alpha\alpha'}^{(j)} - \delta_{\alpha\alpha'} S_{\beta'\beta}^{(j)})$ . Correspondingly,  $\gamma_1$  and  $\gamma_2$  are the single-atom spontaneous decay rates on  $|3\rangle \rightarrow |1\rangle$  and  $|3\rangle \rightarrow |2\rangle$  atomic transitions.

*Results and feasible applications:* In the following, we shall use Eq. (1) to investigate the collective dynamics of an initially excited ensemble of  $\Lambda$ -type emitters when  $\gamma_1 \gg \gamma_2$ .

*Single-atom case:* For the sake of comparison, we first consider a single-atom case. The spontaneous decay law of an initially excited atom is given by the expression

$$\langle S_{33}(t) \rangle = \langle S_{33}(0) \rangle \exp[-2(\gamma_1 + \gamma_2)t], \quad (2)$$

where  $\langle S_{33}(0) \rangle$  denotes the initial population on the  $|3\rangle$  level. This means that in the case of fully excited atom there is no way to influence the decay law of the upper state via applying a coherent laser field on the lower doublet levels. Furthermore, for a purely spontaneous decaying system the ratio of the lower states populations is:  $\langle S_{11}(t) \rangle / \langle S_{22}(t) \rangle = \gamma_1 / \gamma_2$ , i.e., these states will be spontaneously populated depending on the corresponding decay rates [31]. Respectively, the spontaneous electromagnetic field intensities on these transitions are proportional to the population of the lower states during the spontaneous decay. Applying a coherent laser field on the lower doublet states, while the atom being initially on the upper excited state  $|3\rangle$ , the population among the lower energy-levels will oscillate after a while in the usual way.

*Multi-atom case:* In what follows, we shall see how these processes modify in the case of a collectively interacting atomic ensemble. We shall continue by considering an ensemble of emitters with a higher density, i.e.  $n \sim \lambda_2^{-3}$ , such that the emitters on both involved transitions  $|3\rangle \rightarrow |1\rangle$  and  $|3\rangle \rightarrow |2\rangle$  interact collectively. Here  $\lambda_2$  (or  $\lambda_1$ ) is the corresponding wavelength on transition  $|3\rangle \rightarrow |2\rangle$  ( $|3\rangle \rightarrow |1\rangle$ ). Initially, the emitters are prepared in the excited state  $|3\rangle$  and  $\gamma_1 \gg \gamma_2$ . The dynamics of the cooperative decay on both transitions  $|3\rangle \rightarrow |1\rangle$  and  $|3\rangle \rightarrow |2\rangle$  is obtained with the help of master equation Eq. (1) via decoupling of higher order atomic correlators - an approach valid for  $N \gg 1$  [4]. Particularly, the equations for the population on the states  $\langle S_{\alpha\alpha} \rangle / N = \sum_{j=1}^N \langle S_{\alpha\alpha}^{(j)} \rangle / N$ ,  $\alpha \in \{1, 2, 3\}$ , and the intensity of the superradiant emission  $I_\beta \propto \langle S_{3\beta} S_{\beta 3} \rangle / N^2 = \sum_{j,l=1(j \neq l)}^N \langle S_{3\beta}^{(j)} S_{\beta 3}^{(l)} \rangle / N^2$ ,  $\beta \in \{1, 2\}$ , are governed by the number of collectively interacting emitters  $N$ , some geometrical factors  $\{\mu_1, \mu_2\}$  [3, 4], the decay rates  $\{\gamma_1, \gamma_2\}$ , and the Rabi frequency  $\Omega$ , respectively. To give some clarifications regarding the system of equations used to describe our sample, we present few terms in the equations of motion describing the population in the state  $|1\rangle$  and the intensity on the  $|3\rangle \rightarrow |1\rangle$  transition, namely,  $(d/dt)\langle S_{11} \rangle = \dots \sum_{l,k(l \neq k)}^N \gamma_{kl}^{(1)} \langle S_{31}^{(l)} S_{13}^{(k)} \rangle + \text{H.c.}$ , and  $(d/dt)\langle S_{31} S_{13} \rangle = \dots - \sum_{l,m,n(l \neq m \neq n)}^N \gamma_{ml}^{(1)} \langle S_{31}^{(l)} S_{13}^{(n)} (S_{11}^{(m)} - S_{33}^{(m)}) \rangle - \sum_{l,m,n(l \neq m \neq n)}^N \gamma_{ml}^{(2)} \langle S_{32}^{(l)} S_{13}^{(n)} S_{21}^{(m)} \rangle + \text{H.c.}$ , and so on. Here  $\langle S_{11} \rangle = \sum_{j=1}^N \langle S_{11}^{(j)} \rangle$ , whereas  $\langle S_{31} S_{13} \rangle = \sum_{j \neq l}^N \langle S_{31}^{(j)} S_{13}^{(l)} \rangle$ . One can observe that the equation of motion for a certain-order atomic correlator is represented through higher order ones. To obtain a closed system of equations we decoupled the three-particle correlators as follows:  $\langle S_{31}^{(l)} S_{13}^{(n)} (S_{11}^{(m)} - S_{33}^{(m)}) \rangle \approx \langle S_{31}^{(l)} S_{13}^{(n)} \rangle \langle (S_{11}^{(m)} - S_{33}^{(m)}) \rangle$  and  $\langle S_{32}^{(l)} S_{13}^{(n)} S_{21}^{(m)} \rangle \approx \langle S_{32}^{(l)} S_{13}^{(n)} \rangle \langle S_{21}^{(m)} \rangle$ . The 'strategy' in decoupling procedure consists in trying to get a minimal system of equations of motion for a particular decoupling scheme, i.e., in our case the decoupling is applied on three-particle correlators (one can, for instance, start decoupling the four-particle correlators etc). At the end, we will arrive at a non-linear system of 12 equations of motion, which are solved numerically. This method is widely used to characterize multiparticle ensembles [4], and adequately describes collective intensities, populations, the fast decay etc., in the Dicke model or related systems/modifications.

In the absence of the coherent driving, i.e.  $\Omega = 0$ , the time-evolution of populations on the states  $|1\rangle$ ,  $|2\rangle$  and  $|3\rangle$  as well as the collective intensities on the transitions  $|3\rangle \rightarrow |1\rangle$  and  $|3\rangle \rightarrow |2\rangle$  are presented in Fig. 2(a,b) when  $\gamma_1 \gg \gamma_2$ . One can observe typical superradiant behaviors, that is, the population in the state  $|3\rangle$  will cooperatively decay to the state  $|1\rangle$

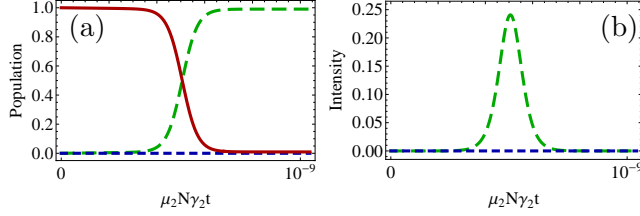


FIG. 2: (Color online) (a) The collective population on the state  $|1\rangle$  (green long-dashed curve), the state  $|2\rangle$  (blue short-dashed line) and the state  $|3\rangle$  (red solid curve) as well as (b) the superradiant intensities on transitions  $|3\rangle \rightarrow |1\rangle$  (green long-dashed curve) and  $|3\rangle \rightarrow |2\rangle$  (blue short-dashed line) as a function of the scaled time  $\mu_2 N \gamma_2 t$ . Here  $\Omega = 0$ ,  $\gamma_2/\gamma_1 = 10^{-8}$ ,  $\mu_2/\mu_1 = 1/16$ ,  $\mu_2 = 10^{-5}$  and  $\langle S_{33}(0) \rangle = N = 10^7$ .

rapidly followed concomitantly by a superradiant pulse emission on transition  $|3\rangle \rightarrow |1\rangle$  (see, respectively, the solid red curve in Fig. 2a and the green long-dashed lines in Fig. 2a and Fig. 2b). However, there is no superradiant emission on transition  $|3\rangle \rightarrow |2\rangle$  (see the blue short-dashed lines in Fig. 2a and Fig. 2b). These behaviors can be well understood in the Dicke limit [4]. For an initially excited large atomic ensemble, i.e.,  $\langle S_{33}(0) \rangle = N$  and  $N \gg 1$ , one has

$$\begin{aligned} \langle S_{11}(t) \rangle + 1 &= (\langle S_{22}(t) \rangle + 1)^{\gamma_1/\gamma_2}, \quad \text{or} \\ \langle S_{22}(t) \rangle + 1 &= (\langle S_{11}(t) \rangle + 1)^{\gamma_2/\gamma_1}. \end{aligned} \quad (3)$$

It is easily to observe that if  $\gamma_1 = \gamma_2$  we always have  $\langle S_{11}(t) \rangle = \langle S_{22}(t) \rangle$ . For longer time-durations and when  $\gamma_1 \ll \gamma_2$  one has that  $\langle S_{11}(t) \rangle \rightarrow 0$  whereas  $\langle S_{22}(t) \rangle \rightarrow N$ , and vice versa, i.e., for  $\gamma_1 \gg \gamma_2$ ,  $\langle S_{22}(t) \rangle \rightarrow 0$  while  $\langle S_{11}(t) \rangle \rightarrow N$ .

Now we add a coherent laser field to couple the lower levels  $|1\rangle \leftrightarrow |2\rangle$ . This transition may be a dipole-forbidden one, therefore, it can be driven via two photon processes. If the Rabi frequency  $\Omega$  is considerably smaller than the collective decay rates, i.e.  $\Omega \ll \mu_1 \gamma_1 N$ , there is only a very small amount of emitters decaying to the ground state  $|2\rangle$  with a weak superradiant burst on transition  $|3\rangle \rightarrow |2\rangle$ , somehow similar to the picture described above. However, when the Rabi frequency is comparable but still smaller than the collective decay rate, i.e.  $\Omega < \mu_1 \gamma_1 N$ , the population dynamics is quite different from the case of smaller Rabi frequencies. Particularly, Figure 3(a,b) depicts the evolution of collective populations in the states  $|1\rangle$ ,  $|2\rangle$  and  $|3\rangle$ , as well as the intensities of the superradiant emissions for

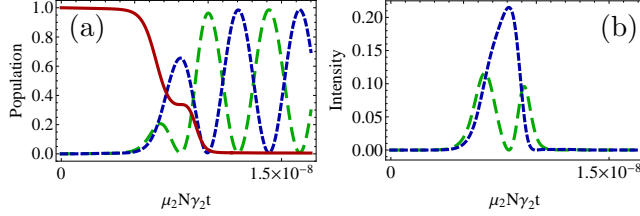


FIG. 3: (Color online) The same as in Fig. 2 but for  $\Omega/(\mu_1\gamma_1N) = 0.47$ .

a particular value of the Rabi frequency, that is for  $\Omega/(\mu_1\gamma_1N) = 0.47$ . Compared with the case  $\Omega = 0$  in Fig. 2(a), the population in the excited state  $|3\rangle$  decreases to zero in a longer time and with a visible small plateau (see the red solid curve in Fig. 3a). On the other side, the population on the state  $|2\rangle$  (blue short-dashed line in Fig. 3a) increases. The superradiance features behave accordingly. Remarkably, there is a strong superradiant pulse occurring on the much weaker transition  $|3\rangle \rightarrow |2\rangle$  (see the blue short-dashed curve in Fig. 3b). Notice that the superradiant behaviors shown in Fig. 3 differ from the ordinary superradiance in the sense that it is not quite determined by the fast population slope of the excited level since, in our case, the excited state population has almost a constant value when the superradiance peak occurs (for two-level emitters the superradiant intensity,  $I$ , is proportional to  $I \propto -\partial\langle S_z(t)\rangle/\partial t$ , where  $\langle S_z(t)\rangle$  is the collective inversion operator). Although the most upper state population has a small plateau during a short time-interval (see the red solid curve in Fig. 3a), the population from the state  $|1\rangle$  transfers, respectively, to  $|2\rangle$  (see the long- and short-dashed curves in Fig. 3a), while the superradiance pulse achieves its maximum on  $|3\rangle \leftrightarrow |2\rangle$  transition (see the blue short-dashed line in Fig. 3b). Furthermore, there are more atoms on the ground state  $|2\rangle$  than in the excited one when the superradiant maximum takes place on the ultraslow transition (see Fig. 3). Again, this is distinct from standard superradiance features found in a two-level sample where the population is distributed equally when the superradiance peak occurs. Further, the intensity on the fast decaying transition vanishes as well as the population in the level  $|1\rangle$  during the superradiant burst on the ultraslow transition (see Fig. 3). Additionally, due to the strong coupling between the states  $|1\rangle$  and  $|2\rangle$ , the superradiant pulse on the fast transition  $|3\rangle \rightarrow |1\rangle$  splits into two pulses (see the green long-dashed curve in Fig. 3b). At final stage, when the population on the state  $|3\rangle$  reduces to zero, Rabi oscillations occur naturally among the states  $|1\rangle$  and  $|2\rangle$ . These behaviors do not change much as long as

$\Omega/(\mu_1\gamma_1N) \sim 1/2$ .

The results described above can be physically explained in the semiclassical dressed-state picture. The corresponding eigenvectors due to laser-dressing of atoms on lower doublet levels can be written in terms of the bare states, namely,

$$|\pm\rangle = \frac{1}{\sqrt{2}} (|2\rangle \pm |1\rangle). \quad (4)$$

The energy difference between the two dressed states depends on the Rabi frequency of the driving coherent laser field  $\Omega$ . The population on the excited state  $|3\rangle$  would decay to the two dressed states  $|\pm\rangle$  which are a mixture of the bare states  $|1\rangle$  and  $|2\rangle$ . Therefore, in the dressed-state picture, the intensity of the superradiant pulses on transitions  $|3\rangle \rightarrow |1\rangle$  and  $|3\rangle \rightarrow |2\rangle$  can be expressed as follows

$$\begin{aligned} I_1 &\propto \langle R_{3-}R_{-3} \rangle + \langle R_{3+}R_{+3} \rangle - \langle R_{3-}R_{+3} \rangle - \langle R_{3+}R_{-3} \rangle, \\ I_2 &\propto \langle R_{3-}R_{-3} \rangle + \langle R_{3+}R_{+3} \rangle + \langle R_{3-}R_{+3} \rangle + \langle R_{3+}R_{-3} \rangle. \end{aligned} \quad (5)$$

Here,  $R_{3\pm} = \sum_{j=1}^N |3\rangle_{jj}\langle\pm|$  ( $R_{\pm 3} = \sum_{j=1}^N |\pm\rangle_{jj}\langle 3|$ ) are the collective transition operators from the dressed states  $|\pm\rangle \rightarrow |3\rangle$  ( $|3\rangle \rightarrow |\pm\rangle$ ) of each emitter  $j$ . It follows from expressions (5) that the intensities of the superradiant pulses, while atoms decay from state  $|3\rangle$  to states  $|1\rangle$  and  $|2\rangle$ , include two parts: one part is the superradiance from state  $|3\rangle$  to the dressed states  $|\pm\rangle$  whereas the other part describes the contribution to the superradiant emission due to quantum coherences among the two decaying paths which are induced by the driving coherent source. When the Rabi frequency  $\Omega$  is large, the emitters in the excited state  $|3\rangle$  would decay via independent channels to the dressed states  $|\pm\rangle$  because the cross-correlations among the two channels average out to zero. However, for smaller Rabi frequency,  $\Omega < \mu_1\gamma_1N$ , the two possible decaying pathways became indistinguishable such that the decay amplitudes from the excited state  $|3\rangle \rightarrow |\pm\rangle$  interfere with each other. These collective decay-induced coherences may give rise to quantum interference between the two decaying paths. Actually, those decay-induced coherences lead to the constructive quantum interference on transition  $|3\rangle \rightarrow |2\rangle$  whereas to destructive quantum interference on transition  $|3\rangle \rightarrow |1\rangle$ , respectively. That is why, for smaller Rabi frequencies, i.e.  $\Omega = 0.47\mu_1\gamma_1N$ , a strong superradiant emission occurs on much weaker transition  $|3\rangle \rightarrow |2\rangle$ , while the superradiant pulse on transition  $|3\rangle \rightarrow |1\rangle$  splits into two pulses. Respectively, the induced quantum



coherences are responsible for population transfer among the lower doublet levels when the superradiant burst takes place, while the higher upper state population is almost constant. The whole cooperative process lasts during a time-period determined by the inverse of the faster collective decay rate. Notice that the cross-correlations among the two involved decay channels in the expressions (5) vanish for a single-atom system (or many independent emitters), i.e.,  $R_{3-}R_{+3} = |3\rangle\langle -||+\rangle\langle 3| = 0$ ,  $R_{3+}R_{-3} = (R_{3-}R_{+3})^\dagger$ , when  $N = 1$ . Therefore, the effect described here is purely of the collective nature. Now we would like to compare the intensities emitted on ultraweak transition for independent emitters,  $I_{2ind}$ , or collectively interacting ones,  $I_{2col}$ . In the first case the intensity is:  $I_{2ind} \sim \gamma_2 N \langle S_{22} \rangle$ , where  $\langle S_{22} \rangle$  is the mean-value of single-atom population in the state  $|2\rangle$ . Taking into account that for independent or single-atom systems  $\langle S_{22} \rangle / \langle S_{11} \rangle = \gamma_2 / \gamma_1$  one has that  $\langle S_{22} \rangle = (\gamma_2 / \gamma_1) / (1 + \gamma_2 / \gamma_1)$ . Thus, in this case,  $I_{2ind} = \gamma_2 N (\gamma_2 / \gamma_1) / (1 + \gamma_2 / \gamma_1)$ . For  $\gamma_2 / \gamma_1 = 10^{-8}$  and  $N = 10^7$ , we have that  $I_{2ind} = 0.1 \gamma_2$ . For a collectively interacting ensemble, the peak intensity on ultraweak transition  $|3\rangle \rightarrow |2\rangle$  can be estimated as:  $I_{2col} \sim \gamma_2 \mu_2 N^2$ . For the same parameters as in Fig. 3(b), one has that:  $I_2 = 20 \gamma_2 N$  which is significantly bigger than that for an independent atomic ensemble.

To create population inversions up to moderate x-rays frequencies may not be principally too hard because of available coherent light sources. Therefore, in these frequency ranges, our scheme may be applied for cooperative lasing or towards amplifying ultraslow atomic transitions like dipole-forbidden ones or due to parity violating effects [24–26]. Enhancing ultraweak transitions in quantum clock systems may be another option [28, 29]. One may use a Lambda-type system containing ultranarrow optical transitions in alkaline-earth atoms (Sr, Yb, Ca, etc.), for instance [32]. For higher frequency effects it turns out that obtaining population inversion is quite challenging, although, one may proceed in the same vein as it was suggested in [33] to excite high lying energy levels in gamma diapason.

*Summary:* We have investigated the superradiance effect occurring in a closely spaced  $\Lambda$ -type atomic ensemble. The single-atom spontaneous decay rates to the lower doublet states are different. For an initially excited system, the superradiance phenomenon is taking place mainly on the transition possessing a higher spontaneous decay rate. We have found that when a coherent laser field is applied to the lower doublet states, the superradiance is surprisingly enhanced on the much weaker atomic transition. This effect is identified with quantum interference effects among the decaying pathways which are induced by the

presence of the coherent driving and it is not observed (i.e. emission enhancement due to quantum interferences) for a single-atom system or an independent atomic ensemble, respectively. Finally, the scheme works as well when  $\gamma_1 > \gamma_2$  or if  $\omega_{31} \gg \omega_{32}$ .

We have benefited from useful discussions with Christoph H. Keitel, Karen Z. Hatsagortyan, Kilian Heeg, and Jonas Gunst. Also, we are grateful for the hospitality of the Theory Division of the Max Planck Institute for Nuclear Physics from Heidelberg, Germany. Furthermore, N.C. acknowledges the financial support from the National Natural Science Foundation of China (Grant No. 11404142), whereas M.M. acknowledges the financial support by the Max Planck Institute for Nuclear Physics as well as the Academy of Sciences of Moldova (grant No. 15.817.02.09F).

---

\* Electronic address: ni.cui@mpi-hd.mpg.de

† Electronic address: macovei@phys.asm.md

- [1] R. H. Dicke, Coherence in Spontaneous Radiation Processes, *Phys. Rev.* **93**, 99 (1954).
- [2] G. S. Agarwal, *Quantum Statistical Theories of Spontaneous Emission and their Relation to other Approaches* (Springer, Berlin, 1974).
- [3] M. Gross and S. Haroche, Superradiance: An essay on the theory of collective spontaneous emission, *Phys. Rep.* **93**, 301 (1982).
- [4] A.V. Andreev, V. I. Emel'yanov, and Yu. A. Il'inskii, *Cooperative Effects in Optics. Superfluorescence and Phase Transitions* (IOP Publishing, London, 1993).
- [5] Z. Ficek and S. Swain, *Quantum Interference and Coherence: Theory and Experiments* (Springer, Berlin, 2005).
- [6] M. Kiffner, M. Macovei, J. Evers, and C. H. Keitel, Vacuum-Induced Processes in Multilevel Atoms, *Progress in Optics* **55**, 85 (2010).
- [7] J. Peng and G.-x. Li, *Introduction to Modern Quantum Optics*, (World Scientific, Singapore, 1998).
- [8] E. Akkermans, A. Gero, and R. Kaiser, Photon Localization and Dicke Superradiance in Atomic Gases, *Phys. Rev. Lett.* **101**, 103602 (2008).
- [9] B. M. Garraway, The Dicke model in quantum optics: Dicke model revisited, *Phil. Trans. R. Soc. A* **369**, 1137 (2011).

- [10] M. Nagasono, J. R. Harries, H. Iwayama, T. Togashi, K. Tono, M. Yabashi, Y. Senba, H. Ohashi, T. Ishikawa, and E. Shigemasa, Observation of Free-Electron-Laser-Induced Collective Spontaneous Emission (Superfluorescence), *Phys. Rev. Lett.* **107**, 193603 (2011).
- [11] C. Müller, M. A. Macovei, and A. B. Voitkiv, Collectively enhanced resonant photoionization in a multiatom ensemble, *Phys. Rev. A* **84**, 055401 (2011).
- [12] N. ten Brinke, R. Schützhold, and D. Habs, Feasibility study of a nuclear exciton laser, *Phys. Rev. A* **87**, 053814 (2013).
- [13] X. Zhang, and A. A. Svidzinsky, Superradiant control of  $\gamma$ -ray propagation by vibrating nuclear arrays, *Phys. Rev. A* **88**, 033854 (2013).
- [14] E. Wolfe, and S. F. Yelin, Certifying Separability in Symmetric Mixed States of N Qubits, and Superradiance, *Phys. Rev. Lett.* **112**, 140402 (2014).
- [15] D. D. Yavuz, Superradiance as a source of collective decoherence in quantum computers, *J. Opt. Soc. Am. B* **31**, 2665 (2014).
- [16] P. Longo, C. H. Keitel, and J. Evers, Tailoring superradiance to design artificial quantum systems, *Sci. Rep.* **6**, 23628 (2016).
- [17] K. Cong, Q. Zhang, Y. Wang, G. Timothy Noe II, A. Belyanin, and J. Kono, Dicke superradiance in solids, *J. Opt. Soc. Am. B* **33**, C80 (2016).
- [18] C. H. Keitel, M. O. Scully, and G. Süssmann, Triggered superradiance, *Phys. Rev. A* **45**, 3242 (1992).
- [19] V. Kozlov, O. Kocharovskaya, Y. Rostovtsev, and M. Scully, Superfluorescence without inversion in coherently driven three-level systems, *Phys. Rev. A* **60**, 1598 (1999).
- [20] L. Yuan, D. Wang, A. A. Svidzinsky, H. Xia, O. Kocharovskaya, A. Sokolov, G. R. Welch, S. Suckewer, and M. O. Scully, Transient lasing without inversion via forbidden and virtual transitions, *Phys. Rev. A* **89**, 013814 (2014).
- [21] J. Gunst, Y. A. Litvinov, C. H. Keitel, and A. Palfy, Dominant Secondary Nuclear Photoexcitation with the X-Ray Free-Electron Laser, *Phys. Rev. Lett.* **112**, 082501 (2014).
- [22] K. P. Heeg, H.-C. Wille, K. Schlage, T. Guryeva, D. Schumacher, I. Uschmann, K. S. Schulze, B. Marx, T. Kämpfer, G. G. Paulus, R. Röhlberger, and J. Evers, Vacuum-Assisted Generation and Control of Atomic Coherences at X-Ray Energies, *Phys. Rev. Lett.* **111**, 073601 (2013).
- [23] E. Paspalakis, and P. L. Knight, Phase Control of Spontaneous Emission, *Phys. Rev. Lett.*

- 81**, 293 (1998).
- [24] M.-A. Bouchiat, and L. Pottier, Optical Experiments and Weak Interactions, *Science* **234**, I203 (1986).
- [25] M. Gunawardena, and D. S. Elliott, Atomic Homodyne Detection of Weak Atomic Transitions, *Phys. Rev. Lett.* **98**, 043001 (2007).
- [26] K. Tsigutkin, D. Dounas-Frazer, A. Family, J. E. Stalnaker, V. V. Yashchuk, and D. Budker, Observation of a Large Atomic Parity Violation Effect in Ytterbium, *Phys. Rev. Lett.* **103**, 071601 (2009).
- [27] Y. Zhang, U. Khadka, B. Anderson, and M. Xiao, Temporal and Spatial Interference between Four-Wave Mixing and Six-Wave Mixing Channels, *Phys. Rev. Lett.* **102**, 013601 (2009).
- [28] R. Santra, E. Arimondo, T. Ido, C. H. Greene, and J. Ye, High-Accuracy Optical Clock via Three-Level Coherence in Neutral Bosonic  $^{88}\text{Sr}$ , *Phys. Rev. Lett.* **94**, 173002 (2005).
- [29] M. A. Norcia, M. N. Winchester, J. R. K. Cline, and J. K. Thompson, Superradiance on the millihertz linewidth strontium clock transition, *Sci. Adv.* **2**: e1601231 (2016).
- [30] D. Meiser, J. Ye, D. R. Carlson, and M. J. Holland, Prospects for a millihertz-linewidth laser, *Phys. Rev. Lett.* **102**, 163601 (2009).
- [31] G. S. Agarwal and S. Das, Electromagnetic field induced modification of branching ratios for emission in structured vacuum, *New Jr. of Phys.* **10**, 013014 (2008).
- [32] J. G. Bohnet., Z. Chen, J. M. Weiner, K. C. Cox, D. Meiser, M. J. Holland, and J. K. Thompson, A quasi-continuous superradiant Raman laser with  $< 1$  intracavity photon, *EPJ Web of Conferences* **57**, 03003 (2013).
- [33] E. V. Baklanov, and V. P. Chebotaev, Concerning possibility of lasing in the gamma band, *JETP Lett.* **21**, 131 (1975).